

Recovery of the magnetic ordering in $Y_{1-x}Ce_xMn_2$ induced by hydrogen absorption

Jesús Chaboy and Cristina Piquer

Instituto de Ciencia de Materiales de Aragón and Departamento de Física de la Materia Condensada, CSIC-Universidad de Zaragoza, 50009 Zaragoza, Spain

Augusto Marcelli, Maurizio Battisti, and Giannantonio Cibin
INFN, Laboratori Nazionali di Frascati, C.P. 13, 00044 Frascati, Italy

Latchezar Bozukov

Department Solid State Physics, Faculty of Physics, Sofia University, 1126 Sofia, Bulgaria

(Received 22 January 1998)

The substitution of Ce by Y in YMn_2 leads to the destabilization of the Mn magnetic moment and inhibits both the transition to antiferromagnetism and the associated expansion of the crystal cell observed in pure YMn_2 . We show in this work how hydrogen uptake in the $Y_{1-x}Ce_xMn_2$ series gives rise to the recovery of long-range magnetic ordering in these systems. The analysis of magnetic and x-ray-absorption spectroscopy experiments addresses the critical role played by the modification of the Ce electronic state in the stabilization of the Mn magnetic moment through the hybridization changes. [S0163-1829(98)02526-0]

The intermetallic Laves phase RMn_2 (R =rare earth and Y) compounds show a wide variety of magnetic behavior depending upon R . This is due to the competition between the localized and itinerant magnetism associated with the rare-earth and manganese sublattices, respectively. Whereas the rare-earth sublattice orders magnetically at low temperatures, the Mn sublattice appears to be close to a magnetic-nonmagnetic instability. The presence of such instability makes the magnetic properties of RMn_2 compounds very sensitive to external parameters such as applied pressure, applied magnetic field or chemical pressure induced by alloying, YMn_2 being one of the most peculiar compounds with such a composition.

YMn_2 was considered long ago to be a Pauli paramagnet with a temperature-independent magnetic susceptibility.¹ However, further studies showed that this compound antiferromagnetically orders below $T_N \sim 100$ K, the observed magnetic moment of Mn being $2.7\mu_B$.² Moreover, in the paramagnetic phase above T_N , YMn_2 bears all the hallmarks of a weak itinerant antiferromagnet.^{3,4} As a consequence, YMn_2 has been extensively studied in the past years as a model system for investigations of itinerant electron magnetism focused on studies of spin fluctuation effects in metals close to a magnetic instability.⁵⁻⁸

Mondal *et al.* have shown that the substitution of Ce by Y in YMn_2 leads to the suppression of the local magnetic moment at the Mn site and therefore, inhibits the transition to antiferromagnetism at low temperatures.⁹ As cerium doping of YMn_2 leads to the reduction of the crystal cell volume, this behavior was interpreted in terms of the critical-distance model, i.e., the existence of a critical spacing for stability of Mn moments $d_c \sim 2.7$ Å above which the Mn atoms retain a large magnetic moment. However, there are numerous experimental evidences, most of them regarding chemical substitutions, in clear disagreement with the critical-distance model predictions.^{10,11} In a similar way, the changes observed in the magnetic behavior of YMn_2 upon hydrogen

uptake cannot be easily understood within the critical-distance framework. The appearance of ferromagnetism in YMn_2 after hydrogen take up was interpreted as due to the increase of the lattice constant increasing with hydrogen concentration.¹ Nevertheless, the magnetic moment disappears again when the lattice is significantly expanded, i.e., when the distance between the Mn atoms becomes too large. A different explanation of the changes in R -Mn hydrides from paramagnetism to ferromagnetism has been given by Wallace, who proposed that the exchange interaction between the magnetic moments depends strongly on the electron concentration.¹²

Previous theoretical calculations have shown that for YMn_2 the position of the Fermi level (E_F) lies near the minimum of the DOS, so that in this case the (unstable) position of the Fermi level results in a strong influence of small modifications of external parameters into the magnetic properties of these materials.^{13,14} Then, a conciliatory scheme to account for the anomalous behavior of the YMn_2 upon chemical substitution of Mn or interstitial hydrogen doping can be obtained in terms of the interplay of both the increase in the Mn-Mn distance and the electronic modification induced by chemical substitution into the DOS modification.^{15,16}

Trying to obtain a deeper insight into the mechanisms responsible for the unusual response of YMn_2 to external parameters we have tailored a series of $Y_{1-x}Ce_xMn_2$ hydrides. As the electronic state of cerium is very sensitive to hydrogen absorption, the DOS of the system would become even more dependent on the Mn-H hybridization due to the existence of the Mn(3d)-Ce(5d) hybridization.

The $Y_{1-x}Ce_xMn_2$ samples were prepared by high-frequency inductive melting under purified Ar atmosphere, followed by two hours annealing in the same furnace just after the melting stage. Hydrides have been formed by using a conventional volumetric automated experimental setup described elsewhere.¹⁷ Both phase and structural analysis were

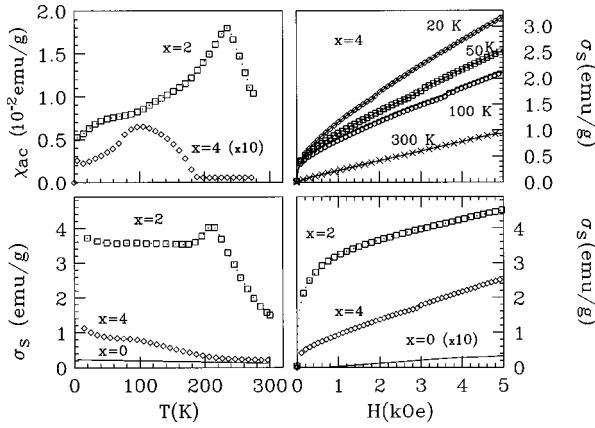


FIG. 1. Left, temperature dependence of the ac susceptibility (top panel) and magnetization (bottom) for the $Y_{0.8}Ce_{0.2}Mn_2H_x$ compounds: $x=0$ (solid line), $x=2$ (\square), and $x=4$ (\diamond). In the right panel magnetization (M) vs applied field (H) at $T=50$ K is shown for the three compounds. In the top panel M vs H plots at different temperatures are shown for $Y_{0.8}Ce_{0.2}Mn_2H_4$.

performed by using a standard x-ray diffractometer. The maximum Ce replacement obtained was $x=0.2$ as determined by means of scanning electron microscopy (SEM). The lattice parameter of $Y_{0.8}Ce_{0.2}Mn_2$ and single-phase $Y_{0.8}Ce_{0.2}Mn_2H_x$ hydrides, x being 2 and the maximum hydrogen concentration ~ 4 H atoms per f.u., are, respectively, 7.653, 8.022, and 8.252 Å.

X-ray-absorption spectroscopy (XAS) experiments were carried out at the ESRF BM29 XAFS beamline 18. The storage ring was operated in 2/3 filling mode with typical currents between 150 and 200 mA at an electron beam energy of 6 GeV. XAS experiments were performed in the transmission mode on homogeneous thin layers of the powdered samples at both Mn K edge and Ce $L_{2,3}$ edges. The fixed-exit double-crystal monochromator was equipped with a pair of Si (111) crystals with an energy resolution $\Delta E/E$ of about 2×10^{-4} . Silicon photodiodes were used to detect the incident and transmitted flux providing a full linear energy response.¹⁸ The absorption spectra were analyzed according to standard procedures: the background contribution from previous edges $\mu_B(E)$ was fitted with a linear function and subtracted from the experimental spectrum $\mu(E)$. Then, spectra were normalized to the absorption coefficient at ~ 100 eV above the edge to eliminate thickness dependence.

The magnetic measurements were performed by using a commercial superconducting quantum interference device magnetometer (Quantum Design MPMS-S5) equipped with an ac susceptibility attachment. The same polycrystalline samples as for the XAS experiments were used. The magnetization of $Y_{0.8}Ce_{0.2}Mn_2$ and its hydride derivatives measured under an applied field of 10 kOe is shown in Fig. 1. The magnetization (M) vs temperature (T) behavior of $Y_{0.8}Ce_{0.2}Mn_2$ corresponds to the existence of a paramagnetic phase in all the temperature range measured, and there is no longer evidence of the antiferromagnetic ordering exhibited by the precursor YMn_2 . The effect of Ce inhibiting the antiferromagnetic ordering in YMn_2 is, however, counteracted by hydrogen absorption. Indeed, the paramagnetic behavior of $Y_{0.8}Ce_{0.2}Mn_2$ is broken after hydrogen uptake, giving rise to a ferrimagnetic behavior below $T \sim 260$ K for $x=2$ and to

weak-ferromagnetism below 200 K for the maximum hydrogen concentration (~ 4 H atom p.f.u.). For $Y_{0.8}Ce_{0.2}Mn_2H_2$ the magnetization reaches a value of $0.12\mu_B$ per Mn atom, under the assumption that neither Y nor Ce carries magnetic moment, while for the $x=4$ hydride the magnetization decreases to only $0.03\mu_B$ per Mn atom. The onset of such a small ferrimagnetic component is made evident for both $x=2$ and 4 $Y_{0.8}Ce_{0.2}Mn_2H_x$ compounds by the magnetic ac susceptibility and magnetization vs applied field measurements shown in Fig. 1.

The magnetic behavior of the Ce doped YMn_2 hydride derivatives resembles that of the pure YMn_2 hydrides. However, the presence of cerium stabilizes the ferrimagnetic regime for the maximum hydrogen concentration whereas in the case of pure YMn_2 the same hydrogen loading leads to the total disappearance of ferrimagnetism. This result casts doubt on the validity of the critical-distance model to account for the magnetic behavior of YMn_2 substitutional derivatives and hydrides. Indeed, according to this model the appearance of ferromagnetism in YMn_2H_x compounds for $2 \leq x \leq 3.5$ is interpreted in terms of the increase of the Mn-Mn interatomic distance, while the loss of the long-range magnetic ordering for further hydrogen charging, YMn_2H_4 , is explained in terms of a large expansion of the crystal-lattice.¹ However, this is not true in the case of the $Y_{0.8}Ce_{0.2}Mn_2$ hydrides showing a markedly different magnetic trend for similar lattice parameters.^{1,19,20} Therefore, to account for this peculiar behavior is necessary to consider the changes induced by the presence of Ce and hydrogen in the electronic structure of this system. Indeed, it has been proposed that the magnetic instability of YMn_2 is linked to the peculiar position of the Fermi level laying near a minimum of the DOS. In particular, Pajda *et al.* have recently revealed the existence of a competition between the Mn-H hybridization, favoring reduced Mn magnetic moments, and the increased lattice constants producing larger Mn moments.¹⁶ Within this framework, the presence of cerium is of particular significance because of the peculiar magnetic behavior of the CeM_2 systems ($M=3d$ transition metal). This depends on the strength of the hybridization between the d states of the transition metal and the cerium $4f$ and $5d$ states.²¹ The high sensitivity of both this hybridization and the Ce electronic state to the hydrogen absorption has been determined to play a relevant role in the modification of the magnetic behavior.²²

In order to obtain a deeper insight into the modification of both the cerium electronic state and Ce($4f,5d$)-Mn($3d$) hybridization upon hydrogen uptake we have recorded the x-ray-absorption spectra at the Mn K edge and Ce L_3 edge in the $Y_{0.8}Ce_{0.2}Mn_2H_x$ series. The comparison of the normalized Mn K edge XANES spectra for YMn_2 , $Y_{0.8}Ce_{0.2}Mn_2$, and $Y_{0.8}Ce_{0.2}Mn_2H_2$ is shown in Fig. 2. The first qualitative inspection of the spectra shows that the YMn_2 crystal structure is retained upon Ce doping. However, there is a marked difference regarding the steplike feature appearing at the edge region that reflects the strong electronic perturbation of the system driven by the cerium substitution and the hydrogen uptake. This region of the spectrum not only probes the unoccupied density of states projected at the Mn site, but this steplike feature at the edge is due to the hybridization between the $p-d$ conduction empty states at the Fermi level.²³

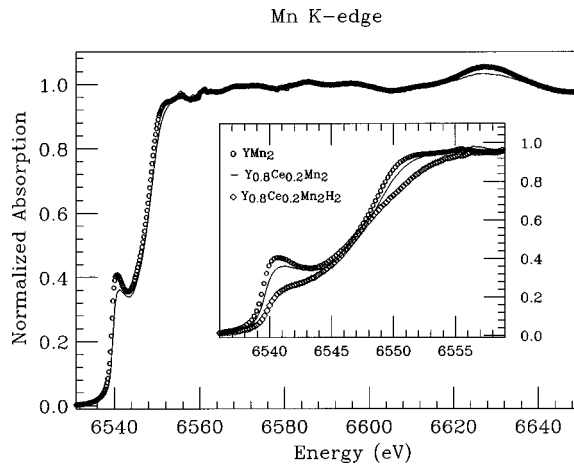


FIG. 2. Comparison between the Mn K edge XANES spectra of YMn_2 (dots) and $\text{Y}_{0.8}\text{Ce}_{0.2}\text{Mn}_2$ (solid line). The inset show a detailed view of the near-edge region, including also the Mn K edge XANES of $\text{Y}_{0.8}\text{Ce}_{0.2}\text{Mn}_2\text{H}_2$ (\diamond).

Because of the Ce($5d$)-M($3d$) hybridization, the intensity of this feature can be correlated to the different role played by both, Ce doping and hydrogen uptake. In the case of $\text{Y}_{0.8}\text{Ce}_{0.2}\text{Mn}_2$ the intensity of this feature shows a 12% reduction and the edge is shifted by 0.2 eV as compared to YMn_2 . The reduction of the intensity of this feature observed as Ce substitutes Y can be explained in terms of the DOS expansion concomitant to the crystal-cell contraction that leads to an enlarged DOS. As in YMn_2 the Fermi level lies near a minimum of the DOS, the expansion shifts the Fermi level towards higher energy and locates it in a region with lower density of states. This fact favors the itinerancy of the system, as is shown by the present experimental results. When hydrogen enters into the $\text{Y}_{0.8}\text{Ce}_{0.2}\text{Mn}_2$ host, there is an expansion of the crystal lattice and an injection of additional electrons to the system. While the first change leads to the narrowing of the DOS, the second implies the progressive filling of the Mn d band. As a consequence the Fermi level shifts slightly upwards so that the DOS at the Fermi level supporting the appearance of ferromagnetism according with the Stoner criterion, and in agreement with the 0.4 eV shift of the Mn K edge observed in $\text{Y}_{0.8}\text{Ce}_{0.2}\text{Mn}_2\text{H}_2$. Moreover, the additional filling of the Mn $3d$ band implies a strong depletion of the d -like empty states above E_F . Then a huge reduction of the shoulderlike feature at the absorption threshold is expected, as found in the case of $\text{Y}_{0.8}\text{Ce}_{0.2}\text{Mn}_2\text{H}_2$, for which the intensity reduction reaches a 40%. As stated above, such edge-structure is due to the hybridization between the p - d conduction empty states at the Fermi level projected on the Mn site. Therefore, because of the strong Ce($4f,5d$)-Mn($3d$) hybridization, characteristic of rare-earth transition-metal intermetallic compounds, we interpret the observed reduction as partially due to the modification of the Ce-Mn hybridization induced by hydrogen. To verify this assignment we have also recorded the Ce L_3 -edge XAS spectra through the series and the results are shown in Fig. 3. In the case of $\text{Y}_{0.8}\text{Ce}_{0.2}\text{Mn}_2$, cerium exhibits the two-peaks profile characteristic of a mixed-valence character, i.e., re-

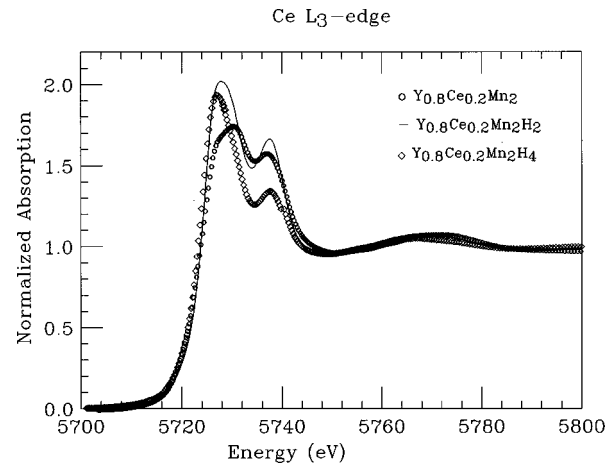


FIG. 3. Comparison between the experimental XANES spectra at the Ce L_3 edge in the case of $\text{Y}_{0.8}\text{Ce}_{0.2}\text{Mn}_2$ (solid line) and their hydride derivatives $\text{Y}_{0.8}\text{Ce}_{0.2}\text{Mn}_2\text{H}_x$, x being 2 (\circ) and 4 (\diamond).

flecting the existence of both the $4f^1$ and $4f^0$ configurations in the initial state,²⁴ in agreement with the observed reduction of the crystal-lattice parameters. Upon hydriding significant changes are found on the intensity, width and relative energy position of the two white lines. The estimate of the Ce valence obtained through the deconvolution of absorption spectra performed according standard methods^{22,24} indicates that the Ce valence decreases from the initial value of 3.40 in $\text{Y}_{0.8}\text{Ce}_{0.2}\text{Mn}_2$ to 3.33 and 3.23 for the hydrides with $x=2$ and 4, respectively. Therefore, although the mixed-valence behavior is retained in all these systems, there is a change of the localization of cerium and consequently the Ce-Mn hybridization is certainly affected by hydrogen uptake. For $\text{Y}_{0.8}\text{Ce}_{0.2}\text{Mn}_2\text{H}_2$ the maximum of the first peak is shifted to low energies by 2.7 eV relative to that of $\text{Y}_{0.8}\text{Ce}_{0.2}\text{Mn}_2$ and its intensity is increased by 15%. This result is a clear indication of the increase of the localization of the Ce-($5d,4f$) band and the subsequent weakening of the Ce-Mn hybridization. Therefore the localized character of the system is reinforced by hydrogen absorption favoring the onset of ferrimagnetism, in agreement to the Mn K edge data. A similar picture is obtained in $\text{Y}_{0.8}\text{Ce}_{0.2}\text{Mn}_2\text{H}_4$ compounds. However, it has to be noted that the increase of the first peak height is only of the 10%, indicating that despite the localization is also favored with respect to the $\text{Y}_{0.8}\text{Ce}_{0.2}\text{Mn}_2$ case, the effect is smaller than for $\text{Y}_{0.8}\text{Ce}_{0.2}\text{Mn}_2\text{H}_2$, in agreement with the transition from ferrimagnetism to weak ferromagnetism observed for the $x=2$ and $x=4$ hydrides, respectively.

In summary we have shown that while the substitution of Ce for Y in YMn_2 leads to the destabilization of the Mn magnetic moment in YMn_2 , long-range magnetic ordering is recovered in $\text{Y}_{1-x}\text{Ce}_x\text{Mn}_2$ after hydrogen absorption. Contrary to the case of the YMn_2 hydrides, magnetic ordering still holds for the maximum hydrogen concentration, indicating the critical role played by cerium, through the Ce-Mn hybridization and its modification with hydrogen uptake into the stabilization of the Mn magnetic moment.

This work was partially supported by the INFN-CICYT agreement and by Spanish DGICYT Grant Nos. MAT96-

0448 and MAT96-0491. The experimental work at the European Synchrotron Radiation Facility was performed with the approval of the European Synchrotron Radiation Facility (ESRF) Program Advisory Committee (Proposal No. HE-

008). We are indebted to A. Filipponi and P. Loeffen for the technical support during the XAS measurements at the ESRF. We wish to thank M.R. Ibarra for many friendly and fruitful discussions.

-
- ¹K. H. J. Buschow and R. C. Sherwood, *J. Appl. Phys.* **48**, 1480 (1978).
- ²Y. Nakamura, M. Shiga, and S. Kawano, *Physica B* **120**, 212 (1983).
- ³M. Shiga, H. Wada, and Y. Nakamura, *J. Magn. Magn. Mater.* **31-34**, 119 (1983).
- ⁴T. Freltoft, P. Boni, G. Shirane, and K. Motoya, *Phys. Rev. B* **37**, 3454 (1988).
- ⁵R. Ballou, J. Deportes, R. Lemaire, Y. Nakamura, and B. Oulad-diaf, *J. Magn. Magn. Mater.* **70**, 129 (1987).
- ⁶H. Imai, H. Wada, and M. Shiga, *J. Phys. Soc. Jpn.* **64**, 2198 (1995).
- ⁷C. Lacroix, A. Solontsov, and R. Ballou, *Phys. Rev. B* **54**, 15 178 (1996).
- ⁸K. Terao, *J. Phys. Soc. Jpn.* **66**, 1796 (1997).
- ⁹S. Mondal, S. H. Kilcone, R. Cywinski, B. D. Rainford, and C. Ritter, *J. Magn. Magn. Mater.* **104-107**, 1421 (1992).
- ¹⁰H. Nakamura, H. Wada, K. Yoshimura, M. Shiga, Y. Nakamura, J. Sakurai, and Y. Komura, *J. Phys. F* **18**, 981 (1988).
- ¹¹M. Shiga, H. Wada, H. Nakamura, K. Yoshimura, and Y. Nakamura, *J. Phys. F* **17**, 1781 (1987).
- ¹²W. E. Wallace, *Z. Phys. Chem., Neue Folge* **115**, 219 (1979).
- ¹³K. Terao and M. Shimizu, *Phys. Lett.* **95A**, 111 (1983); **104A**, 113 (1984).
- ¹⁴H. Yamada, J. Inoue, K. Terao, S. Kanda, and M. Shimizu, *J. Phys. F* **14**, 1943 (1984).
- ¹⁵J. Chaboy, A. Marcelli, M. R. Ibarra, and A. del Moral, *Solid State Commun.* **91**, 859 (1994).
- ¹⁶M. Padjja, R. Ahuja, B. Johansson, J. M. Wills, H. Figiel, A. Paja, and O. Eriksson, *J. Phys.: Condens. Matter* **8**, 3373 (1997).
- ¹⁷L. Bozukov, A. Apostolov, and M. Stoytchev, *J. Magn. Magn. Mater.* **101**, 355 (1991).
- ¹⁸J. Goulon, N. B. Brookes, C. Gauthier, J. Goedkoop, C. Goulon-Ginet, M. Hagelstein, and A. Rogalev, *Physica B* **208&209**, 199 (1995).
- ¹⁹H. Fujii, M. Saga, and T. Okamoto, *J. Less-Common Met.* **130**, 25 (1987).
- ²⁰K. Fujiwara, *J. Phys. Soc. Jpn.* **57**, 2133 (1988).
- ²¹L. Severin and B. Johansson, *Phys. Rev. B* **50**, 17 886 (1994).
- ²²J. Chaboy, A. Marcelli, and L. Bozukov, *J. Phys.: Condens. Matter* **7**, 8197 (1995).
- ²³A. Bianconi, in *X-ray Absorption: Principles, Applications, Techniques of EXAFS, SEXAFS and XANES*, edited by D.C. Koningsberger and R. Prins (Wiley, New York, 1988), Chap. 11, and references therein.
- ²⁴J. Röhler, *J. Magn. Magn. Mater.* **47&48**, 175 (1985).